

Article

Assessment of Machine Learning Algorithms for Predicting Air Entrainment Rates in a Confined Plunging Liquid Jet Reactor

Asmaa Alazmi ¹ and Bader S. Al-Anzi ^{2,*} 

¹ Department of the Construction Project, Ministry of Public Works of Kuwait, Kuwait City 12011, Kuwait; engine85er@vt.edu

² Department of Environmental Technology Management, Kuwait University, P.O. Box 5969, Safat 13060, Kuwait

* Correspondence: bader.alanzi@ku.edu.kw; Tel.: +965-978-85589

Abstract: A confined plunging liquid jet reactor (CPLJR) is an unconventional efficient and feasible aerator, mixer and brine dispenser that operates under many operating conditions. Such operating conditions could be challenging, and hence, utilizing prediction models built on machine learning (ML) approaches could be very helpful in giving reliable tools to manage highly non-linear problems related to experimental hydrodynamics such as CPLJRs. CPLJRs are vital in protecting the environment through preserving and sustaining the quality of water resources. In the current study, the effects of the main parameters on the air entrainment rate, Q_a , were investigated experimentally in a confined plunging liquid jet reactor (CPLJR). Various downcomer diameters (D_c), jet lengths (L_j), liquid volumetric flow rates (Q_j), nozzle diameters (d_n), and jet velocities (V_j) were used to measure the air entrainment rate, Q_a . The non-linear relationship between the air entrainment ratio and confined plunging jet reactor parameters suggests that applying unconventional regression algorithms to predict the air entrainment ratio is appropriate. In addition to the experimental work, machine learning (ML) algorithms were applied to the confined plunging jet reactor parameters to determine the parameter that predicts Q_a the best. The results obtained from ML showed that K-Nearest Neighbour (KNN) gave the best prediction abilities, the proportion of variance in the Q_a that can be explained by the CPLJR parameter was 90%, the root mean square error (RMSE) = 0.069, and the mean absolute error (MAE) = 0.052. Sensitivity analysis was applied to determine the most effective predictor in predicting Q_a . The Q_j and V_j were the most influential among all the input variables. The sensitivity analysis shows that the lasso algorithm can create an effective air entrainment rate model with just two of the most crucial variables, Q_j and V_j . The coefficient of determination (R^2) was 82%. The present findings support using machine learning algorithms to accurately forecast the CPLJR system's experimental results.

Keywords: air entrainment; confined plunging jet; liquid jet reactor; reactor parameters; machine learning algorithms



Citation: Alazmi, A.; Al-Anzi, B.S. Assessment of Machine Learning Algorithms for Predicting Air Entrainment Rates in a Confined Plunging Liquid Jet Reactor. *Sustainability* **2023**, *15*, 13802. <https://doi.org/10.3390/su151813802>

Academic Editor: Agostina Chiavola

Received: 1 August 2023

Revised: 8 September 2023

Accepted: 11 September 2023

Published: 15 September 2023



Copyright: © 2023 by the authors. Licensee MDPI, Basel, Switzerland. This article is an open access article distributed under the terms and conditions of the Creative Commons Attribution (CC BY) license (<https://creativecommons.org/licenses/by/4.0/>).

1. Introduction

The aeration procedure is crucial in mitigating the environmental impact of the discharge of pollutants in different water bodies (e.g., rivers, lakes, ambient seawater and wastewater). Aerators are utilized in a variety of processes, such as aerobic wastewater treatment, air pollution abatement, froth flotation and fermentation. Examples of conventional aerators are diffusers for submerged aeration machines and mechanical surface aerators for the dispersion of atmospheric oxygen into the sewerage water surface. Sewage treatment utilizing natural techniques is a perceived strategy where an aeration system distributes oxygen into wastewater to deliver the oxygen needs of microbes for natural matter oxidation. In general, the presence of a huge air–water interfacial area causes the air to absorb atmospheric oxygen, generating huge instability in the liquid with the emergence

of a submerged two-phase zone, and the oxygen is subsequently distributed into the liquid body via diffusion and convection.

One of the efficient and viable unconventional aerators that has been in use for several decades is the plunging liquid jet reactor (PLJR). A plunging liquid jet can offer robust gas–liquid interaction and the distribution of fine bubbles in liquid while increasing the mass transfer rate by increasing the gas–liquid interfacial area. As a result, this technique can be used to bring air into a body of water, control the oxygen concentration, and mix the water efficiently at low capital and operating cost [1]. Plunging jets can be operated either as unconfined or confined systems.

Because of their low installation, operating, and maintenance expenses, jet aerators are an effective alternative for processing biological liquid waste [2,3]. A jet is intended to plunge through the headspace and impinge on a pool of receiving water that collects a substantial amount of ambient air. A PLJR creates vast and rigorous agitation (determined by the operating conditions) of the water and the entrained bubbles at and below the water surface, which leads to higher oxygen transfer and a well-mixed zone at lower energy consumption.

There have been numerous research studies on the impact of jet variables in plunging jets on water oxygenation effectiveness. Harby et al. (2014), Qu et al. (2011), Al-Anzi (2006), and Van de Sande and Smith (1975) looked at the oxygen transfer from bubbles below the water's surface caused by the effect of a plunging water jet [3–6]. Tojo and Miyunami (1982) explained the mass transfer properties of a gas–liquid jet mixer with cylindrical and rectangular tanks by employing a downflow jet or an up-flow jet [7]. Bagatur et al. (2002) tested numerous nozzle shapes and a 45° penetration slope, finding that the expansion of a water jet with a lesser depth of penetration and rounded nozzle end resulted in the significantly greater absorption of air and oxygen transfer ability than rectangular, elliptical, and circular nozzles due to water jet expansion [8]. In the research by Baylar and Emiroglu (2003), Emiroglu and Baylar (2003) and Ohkawa et al. (1986), the water jet expansion, air entrainment rate, depth of penetration, and oxygen transfer performance of various shaped nozzles with air holes at varied places were examined [9–11]. S Ranjan (2008) and Subodh Ranjan (2007) conducted research on expansion and hollow jet aerators [12,13]. Deswal (2011a) explored the capability of supporting vector machines (SVMs) and Gaussian process regression methods to demonstrate the overall volumetric transfer coefficient of numerous plunging jet frameworks, and He recommended that the SVM method functions admirably by both exact connections, and a Gaussian process could be utilized efficiently in oxygen transfer modelling [2]. Some studies utilized artificial neural network (ANN) and Gaussian process network (GPN) methods to show Q_a by plunging jets, contrasting these demonstrative strategies, exploratory information, and consequences of multiple linear regression (MLR)/multiple non-linear regression (MNLR) and different conditions existing in previous studies. After sensitivity evaluation, the d_n was shown to be the most important parameter on the volumetric Q_a with water jet variables [14,15]. The studies show that the reactor parameters affect the aeration performance in the PLJR. Experimental research shows that even if new devices are incorporated into the PLJR, the new device parameters still affect the net air entrainment rate Q_{anet} . Al-Anzi and Fernandes (2023) incorporated a newly invented Al-Anzi disentrainment ring (ADR) device with a CPLJR to investigate the Q_{anet} enhancement [16]. The results showed that the ADR new variables (length between ADR and receiving pool d_s and ADR length l_{ADR}) positively impacted the Q_{anet} ; for the same ADR device, shorter d_s and l_{ADR} produced higher Q_{anet} .

For decades, the plunging jet reactor model has been applied to induce gas bubble entrainment into a liquid to produce maximum mass transfer rates while maintaining low capital and operational expenses [1]. The application of ML algorithms in CPLJRs remains an interesting part of research due to the gap in the literature concerning the application of ML in CPLJRs. Therefore, it is essential to define the most critical plunging jet parameter that influences the final outcome results, enabling designers to select the best parameters

to provide maximum air entrainment, and thus increase the oxygen mass transfer with a satisfactory power input.

The treatment of wastewater is an important step in reducing aqueous pollution and improving water quality. The configuration of the wastewater specification is extremely diverse, with influent qualities, pollutant concentrations, and treated effluents differing dramatically amongst wastewater treatment plants (WWTPs) [17]. WWTPs are complicated, non-linear systems which have large swings in pollutant load, flow ratio, chemical environment, and hydraulic characteristics. Modelling WWTP procedures is difficult due to these complications and uncertainty [18,19]. Activated sludge models (ASMs) and other biological models have been extensively utilized to evaluate WWTP operations and estimate the behaviour of multiple factors [20–23].

Nevertheless, mechanistic models require a lot of assumptions and explanations to be workable and consistent; hence, they have a lot of constraints; for example, ASMs are only valid under specified temperature, pH, and alkalinity limits. Furthermore, due to variations in methodologies used to calculate state variables, linking multiple mechanistic models that replicate processes in different units is difficult; for example, Total Suspended Solids (TSSs) is calculated and included uniquely in ASMs and second clarifier models [24]. Other inherent flaws of mechanistic models include difficulty in thoroughly replicating multiple processes, significant costs, and poor generalization performance [25]. Because they are entirely dependent on finding correlations between output and input data that allow projections and/or assist decisions, ML models overcome many of these restrictions [26]. The fact that ML models represent real reaction/process conditions rather than mechanisms defined in advance relying on core concepts is a significant advantage. As a result, they are reliable and thorough, which is significant because many of the processes entangled in wastewater treatment are still unknown [27,28]. As a result, the ML modelling of WWTPs is commonly employed as an alternative to mechanistic modelling [25,29,30]. The effect of ambient factors on the adsorption of malachite green (MG) dye from aqueous solutions was optimized using an ANN technique [31]. The outcomes demonstrated the ANN tool's suitability for accurately describing the MG adsorption data.

In WWTPs, several researchers have been working on long-term wastewater regulation [32–34]. ML technology has the potential to recover clean water, electricity, and different elements from wastewater. Wastewater treatment could enhance environmental quality and offer potential economic advantages while also saving water [35]. The wastewater treatment ability achieved by contact aeration for groundwater recharge was evaluated using a known neural network model [36]. The rainfall index was used as a valuable input in the model to improve the economic viability of wastewater treatment, and decisions were made based on the climatic conditions. Akhoundi and Nazif (2018) selected wastewater treatment applications and treatment technologies using evidence-based argumentation approaches [37]. Agricultural irrigation, artificial groundwater recharge, and industrial applications were the most common uses for wastewater treatment—the evidence-based reasoning strategy allowed for a coordinated and complete assessment of wastewater treatment feasibility.

Kumar et al. (2022) investigated the relationships between the variables of plunging hollow jet aerators (discharge, jet thickness, V_j , L_j , depth of water pool, pipe outlet diameter, and number of jets) and the volumetric oxygen transfer coefficient (KLa) [38]. They used techniques from the ANN, SVM, M5 tree (M5), and random forest (RF) families. The outcomes of these ML models are compared next. The results from the SVM were superior. ANNs are a popular ML technique that is based on biological neurons [39]. ANNs can tackle multivariate non-linear problems when given a suitable training technique and enough data [40]. ANNs are also widely used in methodological approaches to eliminate pollutants from water and wastewater. To build black-box representations of systems, ANNs use extremely simplified models made from multiple processing elements—artificial neurons—connected by links of variable weight. Each neuron takes input signals from other neurons, analyses them, and gives out the result, which is then passed on to succeeding

neurons as an input [41]. ANNs adapt from training data and record data point connections, which can then be utilized for modelling, predicting, and optimization. ANNs are ML systems that look like the human brain [42]. They range from simple single-direction logic networks with only one or two layers to complicated multi-input networks with many directional feedback loops and layers. Popular Kernel Function (RBF), Multilayer Perceptron (MLP), Feedforward Neural Network (FNN), Wavelet Neural Network (WNN), self-organizing Map (SOM), Edited Nearest Neighbour (ENN), Recurrent Neural Network (RNN), and deep learning network are some of the ANNs that can be utilized to create models and evaluate the wastewater treatment procedure.

Fuzzy Learning (FL), genetic algorithm (GA), and Evolution Strategies (ES) are examples of single artificial intelligence (AI) technologies in addition to ANNs. FL was created to model complicated and uncertain systems, and it is made up of four parts; fuzzification, defuzzification, and fuzzy rules are all terms used to describe the fuzzy information system [43]. The Fuzzy Inference System (FIS), which comprises four parts—fuzzifier, inference engine, knowledge base, and defuzzifier—is the most extensively employed [44]. The GA, or evolutionary algorithm, models the natural evolutionary procedure to attain the lowest or greatest objective function using Darwin's theory [45]. The Expert System (ES) can replicate the decision-making procedure to resolve complicated problems by combining the skills and knowledge of several experts in a certain sector [46].

Atypical approaches such as Model Tree (MT), clustering algorithm, Batch-Normalization (BN), Particle Swarm Optimization (PSO), and SVM are included in ML technology. By separating the input into subdomains and using a linear multivariate regression model for those subdomains, the MT model can be utilized to address continuous class problems. It can also generate a structural description of the dataset by approximating a non-linear relationship with a piecewise linear model [47]. Problems are addressed in DM by breaking them down into subproblems (subdomains) and then integrating the results of these subproblems. Clustering is an unsupervised technique of organizing the data based on a similarity metric [48]. As per the concept of aggregation, the clustering method, a quantitative multivariate statistical analysis, arranges the unclassified feature vectors into clusters. A Bayesian belief network (BN) is a directed acyclic graph model with nodes and directed edges between connected nodes [49]. The conditional probability distribution of node association represents each node as a random variable [50]. The PSO is an evolving meta-heuristic algorithm that solves optimization issues by starting with a random solution and iterating until the best answer is found [51]. An SVM is a generalized linear classifier that uses the optimal separation concept of classes to solve the binary classification issue [52]. SVMs and associated algorithms have significantly evolved for use in pattern classification [53].

The ANFIS (a hybrid of the neural and fuzzy approaches) was utilized to improve the efficiency of ANNs even further [54,55]. ANFIS adjusts the premise and concluding parameters using a hybrid of backpropagation and least-squares algorithms, and it can produce "If/Then" rules automatically. ANN-GAS employs a genetic algorithm to iteratively refine the parameters of the neural network and improve its problem-solving ability.

It is impossible to define straightforward functional relationships between the airflow and the hydrodynamic and geometric variables that it depends on because air entrainment in drop shafts is so complex [56]. However, by employing prediction models built on ML techniques, which may deliver trustworthy tools to handle highly non-linear problems pertaining to experimental hydrodynamics, this issue can be properly addressed. The objective of the present investigation was to make use of higher-level ML technology as a way of forecasting the gaseous entrapment ratio. The aim of the current study was to evaluate the use of the selected modelling algorithms in predicting the measured air entrainment rates in a CPLJR system. The method is devoid of the costs that would otherwise be associated with laboratory tests. Furthermore, this study explored the use of sensitivity analysis as a method for determining the key variable whose effect has the greatest impact on the results. The results are expected to aid designers in selecting the

most appropriate parameters that ultimately lead to enhanced entrainment and improve the oxygen transfer ratio with relatively low-power considerations.

2. Material and Methods

2.1. Experimental Work and Data Collection

The confined plunging liquid jet (CPLJ) apparatus utilized to generate the current air entrainment rate (Q_a) is shown in Figure 1, which is similar to the apparatuses used by [1,6]. The main operating conditions used to measure Q_a are jet lengths of $L_j = 0.3$ m and 0.4 m; nozzle diameters $d_n = 0.06$ m, 0.08 m, 0.012 m, 0.012 m, and 0.015 m; downcomer diameters of $D_c = 0.023$ m, 0.038 m, 0.0505 m, 0.071 m, and 0.089 m; and downcomer submergence lengths of $H = 0.3$ m and 0.4 m. The nozzle internal design was similar to that used by [9]. The liquid was recycled from the base of $1.5 \times 0.5 \times 0.5$ m³ reservoir utilizing a centrifugal pump and back into the tank through a conical nozzle with known geometry located at the top of the reservoir [1]. The nozzle was fixed concentrically inside a confining tube (downcomer) to ensure that the liquid jet was in the centre of the confining tube. Part of the downcomer was immersed in the liquid that was measured by H . The liquid/water left the nozzle in the form of liquid jet. As the water jet plunged through the headspace, it entrained air (Q_a) from the surroundings in the downward direction, causing the jet diameter to increase along the L_j at high V_j . When the jet impinged on the receiving pool, the entrained air was broken into fine/primary downward bubbles in the centre of the conical bubble swarm and upward secondary bigger bubbles resulted from the coalescence of primary bubbles. Water flow rate was measured using two rotameters with a maximum flowrate of 25 L/min. Gas/air was fed to the system through a tapping located at the top of the downcomer. The air/gas entrainment rate was measured using a bubble meter connected to the gas feed tapping. A solution of 10% household detergent and 5% glycerine in water was used to generate the soap bubbles inside the bubble meter. As the gas entered the bubble meter, it carried soap bubbles up the bubble meter to measure the gas velocity V_a and hence Q_a . A bubble trap was fixed between the bubble meter and gas feed tapping to prevent the soap from going into the system.

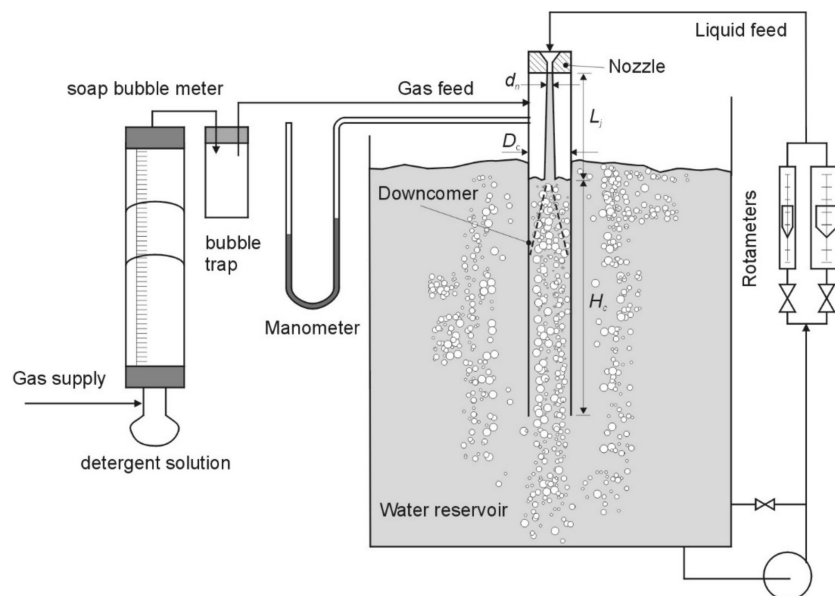


Figure 1. Schematic diagram of the confined plunging liquid jet experimental apparatus [6].

The system measured the net entrainment rate (Q_a), which was the amount of the bubbles leaving the base of the downcomer to aerate the surrounding liquid in the reservoir.

2.2. Dataset

In order to run soft computing models, a total of 353 experimental observations of air entrainment rates were measured by employing a confined plunging liquid jet reactor with variations in jet length L_j (0.3 to 0.4) m, jet velocity V_j (0.9 to 16.3) m/s, jet entrainment rate Q_j (1.46×10^{-5} – 1.91×10^{-3}) m³/s, downcomer diameter D_c (0.023–0.089) m, and nozzle diameter d_n (0.006–0.015) m. The complete experimental observations were divided into two datasets for the training (67% of the data) and testing (33% of the data) of the modelling procedures.

2.3. Modelling

The data were grouped based on a random sample of the total readings. The open-source machine learning toolkit scikit-learn for the Python programming language was used to create each and every regression model. The hyperparameter was tuned using a grid search to define the optimal one. Then, the optimal hyperparameter was used to build the model. Finally, we applied sensitivity analysis to figure out the most critical plunging jet parameter that affected the air entrainment ratio. The permutation importance function from the sklearn library was used to calculate the variable importance of the ML algorithms for our experimental dataset. The permutation feature importance was defined as the drop in model score caused by randomly rearranging a single feature value.

3. Results

Various ML models were established for unique sets of testing and training data, as illustrated in Figure 2. The plots were generated by plotting the air entrainment ratings versus the predicted ratings. The goodness-of-fit (R^2) measure for decision tree (DT), elastic net, extra tree, gradient boosting, K-Nearest Neighbour (KNN), lasso, RF, ridge, and SVM were found to be 0.89, 0.87, 0.87, 0.90, 0.94, 0.83, 0.89, 0.88, and 0.92, respectively. As the R^2 value approached 1, the ML algorithms' predictions of Q_a were efficiently performed when applied to the (CPLJR) parameters.

The produced ML regression model was scored using the evaluation metrics of root mean square error (RMSE) and mean absolute error (MAE). These data were used to determine how accurate our predictions were and how they differed from the actual values. The MAE shows how much of an error from the predicted air entrainment rate was expected on average, and the RMSE shows the average distance between the predicted air entrainment rates from the model and the actual rates in the experimental dataset. The results are summarized in Table 1.

Table 1. Summary of results of the different ML models.

Regressor	MAE	RMSE	R^2
Decision Tree	0.0387	0.0539	0.8931
Elastic Net	0.0442	0.0618	0.8728
Extra Tree	0.0430	0.0598	0.8685
Gradient Boosting	0.1014	0.1255	0.9027
K-Neighbours	0.0271	0.0403	0.9423
Lasso	0.0656	0.0854	0.8279
Random Forest	0.0371	0.0552	0.8873
Ridge	0.0408	0.0581	0.8753
Support Vector Machine	0.0381	0.0484	0.9223

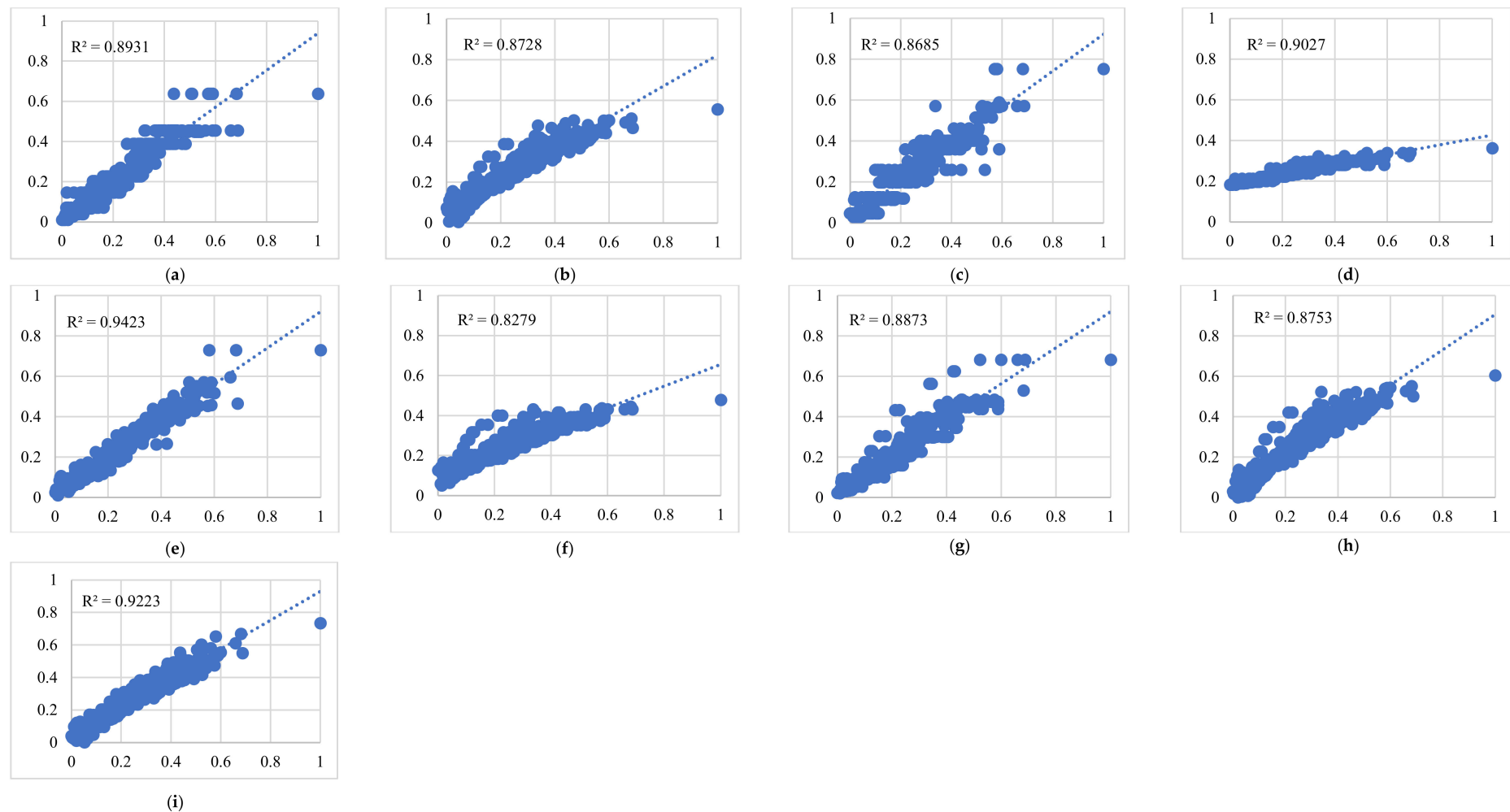


Figure 2. Scatter plots of normalized observed air entrainment via normalized predicted ratings of the machine learning models applied. (a) Air entrainment rate predicted using decision tree; (b) air entrainment rate predicted using elastic net; (c) air entrainment rate predicted using extra tree; (d) air entrainment rate predicted using gradient boosting; (e) air entrainment rate predicted using K-neighbours; (f) air entrainment rate predicted using lasso; (g) air entrainment rate predicted using random forest; (h) air entrainment rate predicted using ridge; (i) air entrainment rate predicted using support vector machine.

Table 1 shows that KNN and RF are the most accurate models that explain the air entrainment rate by the PLJR variables: $R^2 = 0.94$, RMSE = 0.04, and MAE = 0.0271; $R^2 = 0.9223$, RMSE = 0.0484, and MAE = 0.0381. Granata and de Marinis (2017) developed a method based on ML techniques for predicting the Q_a [57]. Three different algorithms were compared in the previous study: M5P, bagging, and RF. The latter definitively outperformed both M5P and bagging; at the same time, the outputs were poor, as seen in the assessment metrics (in the case of RF, the R^2 value was 0.793, while the MAE and RMSE were 0.1406 and 0.2125, respectively). The ML algorithms used in this research are far more accurate than the prior one since this study compares a number of different algorithms.

The aim of this model is to not only build a model with excellent performance but also clarify the model input variables and how these variables affect model performance. A powerful way to define the most critical parameters is by performing a sensitivity analysis on our ML models, where we examine the impact of each parameter on the model's prediction. Figure 3 shows the increase in model RMSE when a single plunging jet reactor parameter value is randomly shuffled. This can tell us which parameter has most impact on the Q_a .

Among all the ML models, the graph shows that the two most important parameters for the models were liquid volumetric flow rate (Q_j) and jet velocity (V_j). The importance of these variables makes sense because when we inverse the V_j , the ore bubbles were transferred to the system. Our findings are in line with previous research performed by Al-Anzi (2020); through his experiment, he found that when the downcomer diameter to nozzle diameter ratio was greater than 5, the highest gas entrainment rates were attained as long as the liquid's surface velocity was high enough to propel bubbles downwards [1].

Furthermore, the ML graphs in Figure 3 maintain the same two important variables. However, the V_j effect decreased in some of the algorithms, such as elastic net, ridge, and SVM. On the other hand, lasso could predict the Q_a when the other variables were shuffled without any root mean square error. The coefficient of determination of the lasso algorithm was 82%. This shows that lasso can build a good model using only the most important variables (Q_j and V_j).

Finally, to obtain a clear overview, we compared the measured, predicted, and calculated Q_a . Figure 4 shows that the fit of the best ML model (KNN) was better than the fit of the Conventional regression model calculated by Al-Anzi (2006) [6]. ML successfully predicted the Q_a using the CPLJR parameters.

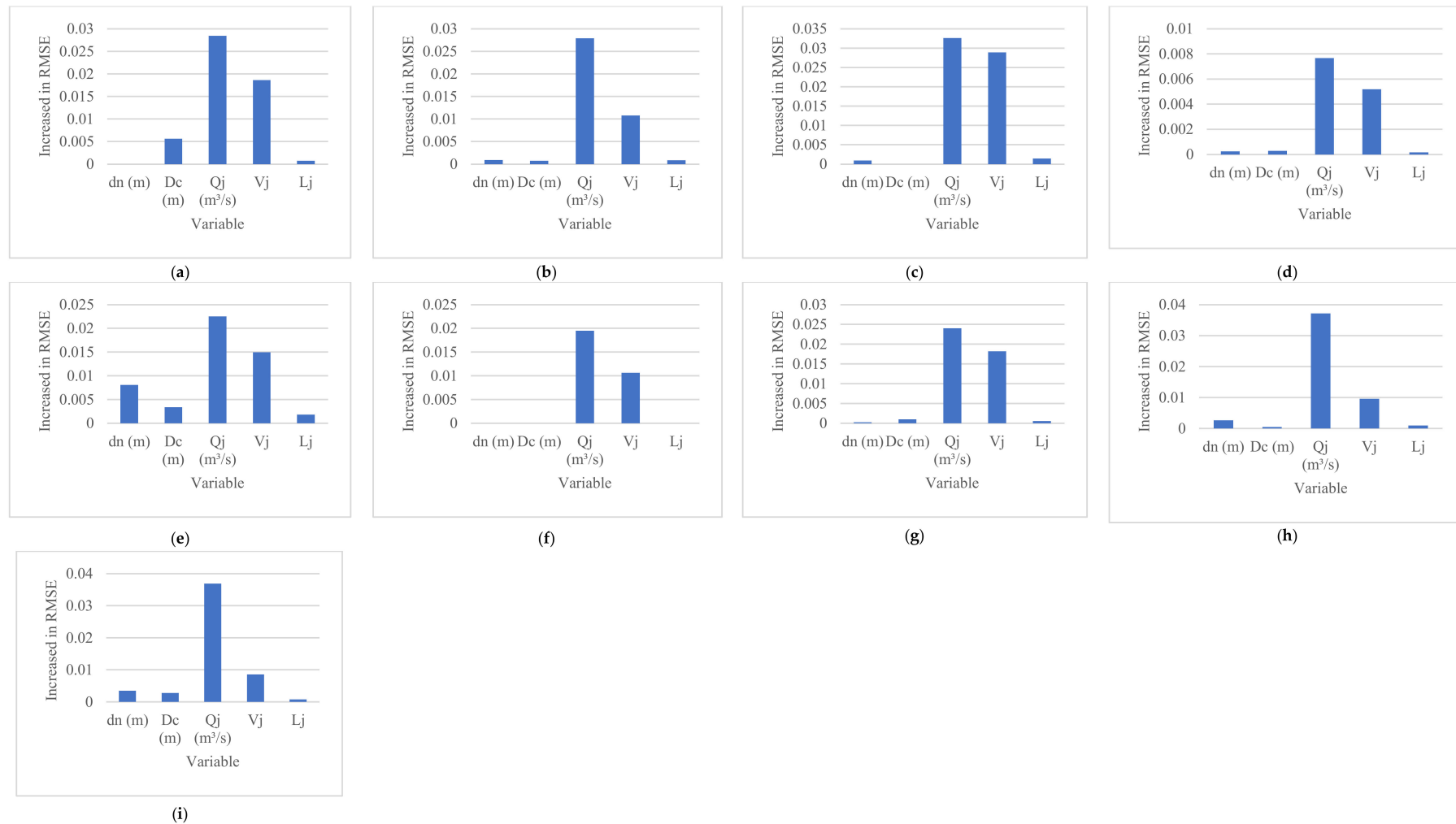


Figure 3. Confined plunging jet reactor parameter level sensitivity analysis graphs of the machine learning models. (a) Decision tree sensitivity analysis; (b) elastic net sensitivity analysis; (c) extra tree sensitivity analysis; (d) gradient boosting sensitivity analysis; (e) K-neighbours sensitivity analysis; (f) lasso sensitivity analysis; (g) random forest sensitivity analysis; (h) ridge sensitivity analysis; (i) support vector machine sensitivity analysis.

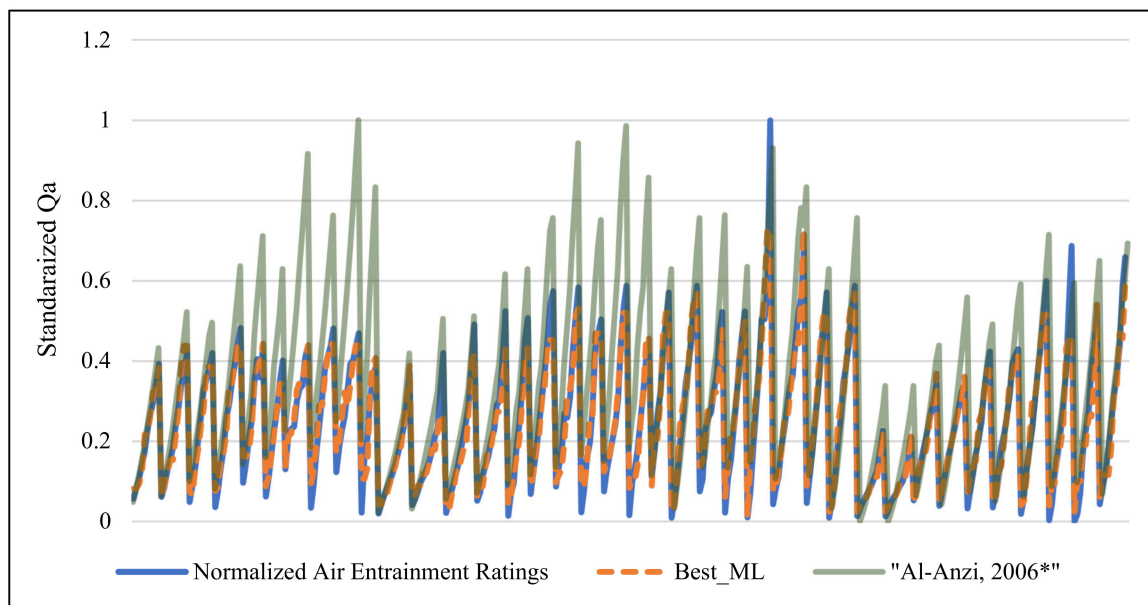


Figure 4. Comparative study between the measured, predicted, and calculated air entrainments rate using Al-Anzi (2006) model * [6].

4. Conclusions

A plunging liquid jet reactor (PLJR), whether a confined or unconfined system, is an unconventional, efficient, and viable aerator and mixer that could be used in many applications to sustain the environment, as indicated in the literature. Such applications are aerobic wastewater treatment processes, fermentation processes, biological aerated filters, the bubble floatation of minerals, chemical stirring, and other applications that require the mixing of gas and liquid phases [1]. The nature of PLJRs enables the rejected brine to be safely discharged into ambient seawater in an optimal manner that simultaneously promotes aeration and dilution at a lower cost. This will increase the dissolved oxygen (DO) concentration levels in the seawater and mix the receiving pool water vigorously to hinder stratification.

A precise prediction of the air entrainment rate in a confined plunging liquid jet reactor is necessary to theoretically determine the operating conditions that play important roles in predicting Q_a accurately and optimally, and at the same time, avoid those that cause an inadequate measurement of the ambient air. A number of machine learning algorithms were compared in this research. All of the models under study demonstrated robustness, dependability, and a strong capacity for generalization. Previous research compared the performance of ML from the families of ANN, SVM, M5 tree (M5), and RF; the results of different ML models were contrasted, and SVM produced better outcomes [38]. However, with reference to the RMSE and R^2 of the ML algorithms applied in this research, KNN and RF presented better performances than the others in predicting an accurate air entrainment rate. ML algorithms might be additionally helpful for giving an assessment of the qualities to be considered for estimating treatment units, given the attributes of the area, when direct methods are not accessible. The projected method could also be compelling with regard to the continuous administration questions of wastewater treatment plants, and it could be utilized to address concerns with environmental planning.

Author Contributions: This work was carried out by A.A. and B.S.A.-A. and reviewed by B.S.A.-A. Conceptualization, A.A. and B.S.A.-A.; methodology, A.A. and B.S.A.-A.; software, A.A.; validation, A.A.; formal analysis, A.A. and B.S.A.-A.; investigation, B.S.A.-A.; resources, B.S.A.-A.; data curation, A.A.; writing—original draft preparation, A.A.; writing—review and editing, B.S.A.-A.; visualization, A.A.; supervision, B.S.A.-A.; project administration, A.A.; funding acquisition, B.S.A.-A. All authors have read and agreed to the published version of the manuscript.

Funding: This research received no external funding.

Institutional Review Board Statement: Not applicable.

Informed Consent Statement: Not applicable.

Data Availability Statement: The data presented in this study are available on request from the corresponding author.

Conflicts of Interest: The authors declare no conflict of interest.

References

1. Al-Anzi, B.S. Effect of Primary Variables on A Confined Plunging Liquid Jet Reactor. *Water* **2020**, *12*, 764. [\[CrossRef\]](#)
2. Deswal, S. Modeling oxygen-transfer by multiple plunging jets using support vector machines and Gaussian process regression techniques. *Int. J. Civ. Environ. Eng.* **2011**, *5*, 1–6.
3. Van de Sande, E.; Smith, J.M. Mass transfer from plunging water jets. *Chem. Eng. J.* **1975**, *10*, 225–233. [\[CrossRef\]](#)
4. Qu, X.; Khezzar, L.; Danciu, D.; Labois, M.; Lakehal, D. Characterization of plunging liquid jets: A combined experimental and numerical investigation. *Int. J. Multiph. Flow* **2011**, *37*, 722–731. [\[CrossRef\]](#)
5. Harby, K.; Chiva, S.; Muñoz-Cobo, J. An experimental study on bubble entrainment and flow characteristics of vertical plunging water jets. *Exp. Therm. Fluid Sci.* **2014**, *57*, 207–220. [\[CrossRef\]](#)
6. Al-Anzi, B.S.; Cumming, I.W.; Rielly, C.D. Air entrainment rates in a confined plunging liquid jet reactor. In Proceedings of the 10th International Conference Multiphase Flow in Industrial Plant, Tropea, Italy, 20–22 September 2006; Volume 1, pp. 71–82.
7. Tojo, K.; Miyanami, K. Oxygen transfer in jet mixers. *Chem. Eng. J.* **1982**, *24*, 89–97. [\[CrossRef\]](#)
8. Bagatur, T.; Baylar, A.; Sekerdag, N. The Effect of Nozzle Type on Air Entrainment by Plunging Water Jets. *Water Qual. Res. J.* **2002**, *37*, 599–612. [\[CrossRef\]](#)
9. Ohkawa, A.; Kusabiraki, D.; Shiokawa, Y.; Sakai, N.; Fujii, M. Flow and oxygen transfer in a plunging water jet system using inclined short nozzles and performance characteristics of its system in aerobic treatment of wastewater. *Biotechnol. Bioeng.* **1986**, *28*, 1845–1856. [\[CrossRef\]](#)
10. Baylar, A.; Emiroglu, M.E. Air entrainment and oxygen transfer in a venturi. *Proc. Inst. Civ. Eng.-Water Marit. Eng.* **2003**, *156*, 249–255. [\[CrossRef\]](#)
11. Emiroglu, M.E.; Baylar, A. Role of Nozzles with Air Holes in Air Entrainment by a Water Jet. *Water Qual. Res. J.* **2003**, *38*, 785–795. [\[CrossRef\]](#)
12. Ranjan, S. Hydraulics of hollow jet aerators. *J. Indian Water Resour. Soc.* **2007**, *27*, 27–31.
13. Ranjan, S. Hydraulics of jet aerators. *J. Inst. Eng. Environ. Eng. Div.* **2008**, *88*, 29–32.
14. Bagatur, T.; Onen, F. A predictive model on air entrainment by plunging water jets using GEP and ANN. *KSCE J. Civ. Eng.* **2014**, *18*, 304–314. [\[CrossRef\]](#)
15. Onen, F. Prediction of penetration depth in a plunging water jet using soft computing approaches. *Neural Comput. Appl.* **2014**, *25*, 217–227. [\[CrossRef\]](#)
16. Al-Anzi, B.S.; Fernandes, J. Measurement of Total Air Entrainment, Disentrainment and Net Entrainment Flow Rates Utilizing Novel Downcomer Incorporating Al-Anzi's Disentrainment Ring (ADR) in a Confined Plunging Jet Reactor. *Water* **2023**, *15*, 835. [\[CrossRef\]](#)
17. Long, S.; Zhao, L.; Liu, H.; Li, J.; Zhou, X.; Liu, Y.; Qiao, Z.; Zhao, Y.; Yang, Y. A Monte Carlo-based integrated model to optimize the cost and pollution reduction in wastewater treatment processes in a typical comprehensive industrial park in China. *Sci. Total Environ.* **2019**, *647*, 1–10. [\[CrossRef\]](#) [\[PubMed\]](#)
18. Rout, P.R.; Zhang, T.C.; Bhunia, P.; Surampalli, R.Y. Treatment technologies for emerging contaminants in wastewater treatment plants: A review. *Sci. Total Environ.* **2021**, *753*, 141990. [\[CrossRef\]](#) [\[PubMed\]](#)
19. Vučić, V.; Süring, C.; Harms, H.; Müller, S.; Günther, S. A framework for P-cycle assessment in wastewater treatment plants. *Sci. Total Environ.* **2021**, *760*, 143392. [\[CrossRef\]](#)
20. Buaisha, M.; Balku, S.; Özalp-Yaman, S. Heavy metal removal investigation in conventional activated sludge systems. *Civ. Eng. J.* **2020**, *6*, 470–477. [\[CrossRef\]](#)
21. Fenu, A.; Guglielmi, G.; Jimenez, J.; Spèrandio, M.; Saroj, D.; Lesjean, B.; Brepols, C.; Thoeye, C.; Nopens, I. Activated sludge model (ASM) based modelling of membrane bioreactor (MBR) processes: A critical review with special regard to MBR specificities. *Water Res.* **2010**, *44*, 4272–4294. [\[CrossRef\]](#)

22. Nopens, I.; Batstone, D.J.; Copp, J.B.; Jeppsson, U.; Volcke, E.; Alex, J.; Vanrolleghem, P.A. An ASM/ADM model interface for dynamic plant-wide simulation. *Water Res.* **2009**, *43*, 1913–1923. [\[CrossRef\]](#)
23. Wu, X.; Yang, Y.; Wu, G.; Mao, J.; Zhou, T. Simulation and optimization of a coking wastewater biological treatment process by activated sludge models (ASM). *J. Environ. Manag.* **2016**, *165*, 235–242. [\[CrossRef\]](#) [\[PubMed\]](#)
24. Metcalf, E.; Tchobanoglous, G.; Stensel, H.D.; Tsuchihashi, R.; Burton, F. *Wastewater Engineering: Treatment and Resource Recovery*; McGraw-Hill: New York, NY, USA, 2013.
25. Cao, W.; Yang, Q. Online sequential extreme learning machine based adaptive control for wastewater treatment plant. *Neurocomputing* **2020**, *408*, 169–175. [\[CrossRef\]](#)
26. Müller, A.C.; Guido, S. *Introduction to Machine Learning with Python: A Guide for Data Scientists*; O'Reilly Media, Inc.: Sebastopol, CA, USA, 2016.
27. Erdirencelebi, D.; Yalpir, S. Adaptive network fuzzy inference system modeling for the input selection and prediction of anaerobic digestion effluent quality. *Appl. Math. Model.* **2011**, *35*, 3821–3832. [\[CrossRef\]](#)
28. Nadiri, A.A.; Shokri, S.; Tsai, F.T.-C.; Moghaddam, A.A. Prediction of effluent quality parameters of a wastewater treatment plant using a supervised committee fuzzy logic model. *J. Clean. Prod.* **2018**, *180*, 539–549. [\[CrossRef\]](#)
29. Liu, H.; Zhang, Y.; Zhang, H. Prediction of effluent quality in papermaking wastewater treatment processes using dynamic kernel-based extreme learning machine. *Process. Biochem.* **2020**, *97*, 72–79. [\[CrossRef\]](#)
30. Shi, S.; Xu, G. Novel performance prediction model of a biofilm system treating domestic wastewater based on stacked denoising auto-encoders deep learning network. *Chem. Eng. J.* **2018**, *347*, 280–290. [\[CrossRef\]](#)
31. Al-Musawi, T.J.; Arghavan, S.M.A.; Allahyari, E.; Arghavan, F.S.; Othmani, A.; Nasseh, N. Adsorption of malachite green dye onto almond peel waste: A study focusing on application of the ANN approach for optimization of the effect of environmental parameters. *Biomass-Convert. Biorefinery* **2023**, *13*, 12073–12084. [\[CrossRef\]](#)
32. Jia, X.; Li, Z.; Tan, R.R.; Foo, D.C.; Majozi, T.; Wang, F. Interdisciplinary contributions to sustainable water management for industrial parks. *Resour. Conserv. Recycl.* **2019**, *149*, 646–648. [\[CrossRef\]](#)
33. López-Morales, C.A.; Rodríguez-Tapia, L. On the economic analysis of wastewater treatment and reuse for designing strategies for water sustainability: Lessons from the Mexico Valley Basin. *Resour. Conserv. Recycl.* **2019**, *140*, 1–12. [\[CrossRef\]](#)
34. Man, Y.; Hu, Y.; Ren, J. Forecasting COD load in municipal sewage based on ARMA and VAR algorithms. *Resour. Conserv. Recycl.* **2019**, *144*, 56–64. [\[CrossRef\]](#)
35. Bozkurt, H.; van Loosdrecht, M.C.; Gernaey, K.V.; Sin, G. Optimal WWTP process selection for treatment of domestic wastewater—A realistic full-scale retrofitting study. *Chem. Eng. J.* **2016**, *286*, 447–458. [\[CrossRef\]](#)
36. Chen, J.; Chang, N.; Shieh, W. Assessing wastewater reclamation potential by neural network model. *Eng. Appl. Artif. Intell.* **2003**, *16*, 149–157. [\[CrossRef\]](#)
37. Akhoundi, A.; Nazif, S. Sustainability assessment of wastewater reuse alternatives using the evidential reasoning approach. *J. Clean. Prod.* **2018**, *195*, 1350–1376. [\[CrossRef\]](#)
38. Kumar, M.; Tiwari, N.K.; Ranjan, S. Application of Machine Learning Methods in Estimating the Oxygenation Performance of Various Configurations of Plunging Hollow Jet Aerators. *J. Environ. Eng.* **2022**, *148*, 04022070. [\[CrossRef\]](#)
39. López, M.E.; Rene, E.R.; Boger, Z.; Veiga, M.C.; Kennes, C. Modelling the removal of volatile pollutants under transient conditions in a two-stage bioreactor using artificial neural networks. *J. Hazard. Mater.* **2017**, *324*, 100–109. [\[CrossRef\]](#)
40. Wang, J.; Deng, Z. Modeling and Prediction of Oyster Norovirus Outbreaks along Gulf of Mexico Coast. *Environ. Health Perspect.* **2016**, *124*, 627–633. [\[CrossRef\]](#)
41. Chakraborty, T.; Chakraborty, A.K.; Chattopadhyay, S. A novel distribution-free hybrid regression model for manufacturing process efficiency improvement. *J. Comput. Appl. Math.* **2019**, *362*, 130–142. [\[CrossRef\]](#)
42. Zhang, Y.; Gao, X.; Smith, K.; Inial, G.; Liu, S.; Conil, L.B.; Pan, B. Integrating water quality and operation into prediction of water production in drinking water treatment plants by genetic algorithm enhanced artificial neural network. *Water Res.* **2019**, *164*, 114888. [\[CrossRef\]](#)
43. Zhao, L.; Dai, T.; Qiao, Z.; Sun, P.; Hao, J.; Yang, Y. Application of artificial intelligence to wastewater treatment: A bibliometric analysis and systematic review of technology, economy, management, and wastewater reuse. *Process. Saf. Environ. Prot.* **2020**, *133*, 169–182. [\[CrossRef\]](#)
44. Chanapathi, T.; Thatikonda, S. Fuzzy-Based Regional Water Quality Index for Surface Water Quality Assessment. *J. Hazardous Toxic Radioact. Waste* **2019**, *23*, 04019010. [\[CrossRef\]](#)
45. Al Aani, S.; Bonny, T.; Hasan, S.W.; Hilal, N. Can machine language and artificial intelligence revolutionize process automation for water treatment and desalination? *Desalination* **2019**, *458*, 84–96. [\[CrossRef\]](#)
46. Wagner, W.P. Trends in expert system development: A longitudinal content analysis of over thirty years of expert system case studies. *Expert Syst. Appl.* **2017**, *76*, 85–96. [\[CrossRef\]](#)
47. Sattar, A.A.; Elhakeem, M.; Rezaie-Balf, M.; Gharabaghi, B.; Bonakdari, H. Artificial intelligence models for prediction of the aeration efficiency of the stepped weir. *Flow Meas. Instrum.* **2019**, *65*, 78–89. [\[CrossRef\]](#)
48. Bagheri, M.; Mirbagheri, S.; Ehteshami, M.; Bagheri, Z. Modeling of a sequencing batch reactor treating municipal wastewater using multi-layer perceptron and radial basis function artificial neural networks. *Process. Saf. Environ. Prot.* **2015**, *93*, 111–123. [\[CrossRef\]](#)

49. Graham, E.S.; Chariton, A.A.; Landis, W.G. Using Bayesian networks to predict risk to estuary water quality and patterns of benthic environmental DNA in Queensland. *Integr. Environ. Assess. Manag.* **2019**, *15*, 93–111. [[CrossRef](#)]
50. Li, D.; Yang, H.Z.; Liang, X.F. Prediction analysis of a wastewater treatment system using a Bayesian network. *Environ. Model. Softw.* **2013**, *40*, 140–150. [[CrossRef](#)]
51. Qiao, Y.; Zhang, S.; Wu, N.; Wang, X.; Li, Z.; Zhou, M.; Qu, T. Data-driven approach to optimal control of ACC systems and layout design in large rooms with thermal comfort consideration by using PSO. *J. Clean. Prod.* **2019**, *236*, 117578. [[CrossRef](#)]
52. Sousa, V.; Matos, J.P.; Matias, N. Evaluation of artificial intelligence tool performance and uncertainty for predicting sewer structural condition. *Autom. Constr.* **2014**, *44*, 84–91. [[CrossRef](#)]
53. Lu, H.; Li, H.; Liu, T.; Fan, Y.; Yuan, Y.; Xie, M.; Qian, X. Simulating heavy metal concentrations in an aquatic environment using artificial intelligence models and physicochemical indexes. *Sci. Total Environ.* **2019**, *694*, 133591. [[CrossRef](#)]
54. Mohandes, M.; Rehman, S.; Rahman, S. Estimation of wind speed profile using adaptive neuro-fuzzy inference system (ANFIS). *Appl. Energy* **2011**, *88*, 4024–4032. [[CrossRef](#)]
55. Yang, Z.; Liu, Y.; Li, C. Interpolation of missing wind data based on ANFIS. *Renew. Energy* **2011**, *36*, 993–998. [[CrossRef](#)]
56. Granata, F.; Di Nunno, F. Air Entrainment in Drop Shafts: A Novel Approach Based on Machine Learning Algorithms and Hybrid Models. *Fluids* **2022**, *7*, 20. [[CrossRef](#)]
57. Granata, F.; de Marinis, G. Machine learning methods for wastewater hydraulics. *Flow Meas. Instrum.* **2017**, *57*, 1–9. [[CrossRef](#)]

Disclaimer/Publisher's Note: The statements, opinions and data contained in all publications are solely those of the individual author(s) and contributor(s) and not of MDPI and/or the editor(s). MDPI and/or the editor(s) disclaim responsibility for any injury to people or property resulting from any ideas, methods, instructions or products referred to in the content.